Miklós KUCZMANN

Széchenyi István University

The polarization method combined with the Newton-Raphson technique in magnetostatic field problems

***Abstract**. Nonlinear magnetic field problems can be solved by using the polarization method. After applying the Finite Element Method (FEM), a system of nonlinear equations can be derived, which can only be solved by iterative techniques. The fixed point iteration scheme and the Newton-Raphson technique are the most widely used algorithms to solve nonlinear equations. The first is known as a convergent, but slow algorithm, while the other is a fast solver, which convergence can be critical. This paper presents and compares the two methods.*

***Streszczenie.** Nieliniowe problemy pola magnetycznego mogą być rozwiązywane przy użyciu metody polaryzacji. Po zastosowaniu MES otrzymuje się system równań nieliniowych, które mogą być rozwiązywane jedynie metodami iteracyjnymi. Schemat iteracyjny ustalonego punktu oraz technika Newtona-Raphsona są najczęściej stosowane w rozwiązywaniu równań nieliniowych. Pierwsze podejście daje algorytm zbieżny ale wolny, drugo zaś daje algorytm szybki ale na granicy zbieżności. W artykule przedstawiono i porównano te dwa podejścia. (**Metoda polaryzacji połączona z techniką Newtona-Raphsona w analizie pola magnetostatycznego**)*

Keywords: Nonlinear magnetic field, FEM, fixed point technique, Newton-Raphson method.
Słowa kluczowe: nieliniowe pole magnetyczne, technika punktu ustalonego, metoda Newtona-Raphsona.

Introduction

Efficient implementation of nonlinear characteristics in electromagnetic field simulation environments is still an open question today. Problems including nonlinear characteristics can only be solved by iterative techniques, when a linearized problem is solved at every iteration step. The most widely used procedure in computational electromagnetism is FEM [1]. The unknowns are associated to the nodes or edges of the mesh. The number of unknowns can be very large, that is why a computationally efficient nonlinear solver must be worked out.

The nonlinear model must simulate the hysteretic behavior as accurately as possible. At the same time it should be realized by a fast algorithm from the computational point of view, since the model is requested many times during the iteration. The model should handle nonphysical values of the magnetic field, too (e.g. in the vicinity of singularities).

The nonlinear characteristics can be handled by the polarization technique, when the magnetic field intensity or the magnetic flux density is split into a linear and a nonlinear part. The nonlinear part is depending on the constitutive relationship, and it is determined iteratively.

The most usual techniques are the fixed point method and the Newton-Raphson method [2,3]. The fixed point algorithm can result in an unconditionally convergent method, which is, however very slow. The Newton-Raphson method is known as a fast iteration scheme, especially when the iterated solution is close to the true one. The behavior of its convergence is sometimes very strange.

Governing equations and applying FEM

Maxwell's equations of the static magnetic field problems are as follows [1]:

(1) $\nabla \times \boldsymbol{H} = \boldsymbol{J}, \ \ \nabla \cdot \boldsymbol{B} = 0, \ \ \text{in} \ \ \Omega_0 \cup \Omega_m$,

where $\boldsymbol{H}$, $\boldsymbol{B}$ and $\boldsymbol{J}$ are the magnetic field intensity, the magnetic flux density and the source current density of the excitation coil, which is supposed to be known here. The constitutive relation between the magnetic field intensity and the magnetic flux density in the air region Ω_0 is $\boldsymbol{H} = \nu_0 \boldsymbol{B}$, where $\nu_0 = 1/\mu_0$ is the inverse of permeability of vacuum. The nonlinear constitutive relationship is represented by a nonlinear model in Ω_m. According to the polarization technique, the magnetic field intensity is split into two parts as [2,3]

(2) $\boldsymbol{H} = \nu \boldsymbol{B} + \boldsymbol{I} \ \ \text{in} \ \ \Omega_\mathrm{m}$.

Here ν is a reluctivity-like quantity, and $\boldsymbol{I}$ is a nonlinear term depending on the input-output state of the applied hysteresis model.

The problem region is surrounded by the boundary $\Gamma_H \cup \Gamma_B$. On Γ_H, the tangential component of $\boldsymbol{H}$, on Γ_B, the normal component of $\boldsymbol{B}$ is set zero, respectively, i.e. $\boldsymbol{H} \times \boldsymbol{n} = \boldsymbol{0}, \text{on}\ \Gamma_H$, and $\boldsymbol{B} \cdot \boldsymbol{n} = 0, \text{on}\ \Gamma_B$.

From $\nabla \cdot \boldsymbol{B} = 0$ in (1), the magnetic vector potential $\boldsymbol{A}$ can be introduced as [1]

(3) $\boldsymbol{B} = \nabla \times \boldsymbol{A}$.

Substituting this relation back to (1) via (2), the nonlinear partial differential equation

(4) $\nabla \times [\nu \nabla \times \boldsymbol{A}] = \boldsymbol{J} - \nabla \times \boldsymbol{I}$

can be obtained, and the boundary conditions of the problem can be formulated as

(5) $[\nu \nabla \times \boldsymbol{A} + \boldsymbol{I}] \times \boldsymbol{n} = \boldsymbol{0}, \ \ \text{on} \ \ \Gamma_H,$ and $\boldsymbol{n} \times \boldsymbol{A} = \boldsymbol{0}, \ \ \text{on} \ \ \Gamma_B$.

The divergence of magnetic vector potential can be selected according to Coulomb gauge, i.e. $\nabla \cdot \boldsymbol{A} = 0$. After some manipulations [1], Coulomb gauge can be enforced as

(6) $\nabla \times [\nu \nabla \times \boldsymbol{A}] - \nabla [\nu \nabla \cdot \boldsymbol{A}] = \boldsymbol{J} - \nabla \times \boldsymbol{I}$.

This results in two more conditions beyond (5),

(7) $\boldsymbol{A} \cdot \boldsymbol{n} = 0, \ \ \text{on} \ \ \Gamma_H,$ and $\nu \nabla \cdot \boldsymbol{A} = 0, \ \ \text{on} \ \ \Gamma_B$.

The partial differential equation (4) with boundary conditions in (5) can be used when approximating $\boldsymbol{A}$ by vector FEM [1]. In this case, $\boldsymbol{J}$ is approximated by the impressed current vector potential $\boldsymbol{T}$, since $\boldsymbol{J} = \nabla \times \boldsymbol{T}$, i.e. (4) has to be changed as

(8) $\nabla \times [\nu \nabla \times \boldsymbol{A}] = \nabla \times \boldsymbol{T} - \nabla \times \boldsymbol{I}$.

Moreover, the partial differential equation (6) with boundary conditions (5) and (7) can be used when approximating $\boldsymbol{A}$ by nodal FEM [1].

After some manipulations, the weak formulation of the ungauged and gauged $\boldsymbol{A}$-formulation can be obtained:

$$\begin{aligned}(9)\quad &\int_\Omega \nabla\times\boldsymbol{W}\cdot\left[\nu\,\nabla\times\boldsymbol{A}\right]\mathrm{d}\Omega = \int_\Omega \nabla\times\boldsymbol{W}\cdot\boldsymbol{T}\,\mathrm{d}\Omega \\ &-\int_\Omega \nabla\times\boldsymbol{W}\cdot\boldsymbol{I}\,\mathrm{d}\Omega,\end{aligned}$$

and

$$\begin{aligned}(10)\quad &\int_\Omega \nabla\times\boldsymbol{W}\cdot\left[\nu\,\nabla\times\boldsymbol{A}\right]+\nabla\cdot\boldsymbol{W}\left[\nu\,\nabla\cdot\boldsymbol{A}\right]\mathrm{d}\Omega = \int_\Omega \boldsymbol{W}\cdot\boldsymbol{J}\,\mathrm{d}\Omega \\ &-\int_\Omega \nabla\times\boldsymbol{W}\cdot\boldsymbol{I}\,\mathrm{d}\Omega,\end{aligned}$$

respectively.

The following functionals are minimized during the nonlinear iteration:

$$\begin{aligned}(11)\quad &F(\boldsymbol{A}) = \frac{1}{2}\int_\Omega \nu\left|\nabla\times\boldsymbol{A}\right|^2\mathrm{d}\Omega - \int_\Omega \nabla\times\boldsymbol{A}\cdot\boldsymbol{T}\,\mathrm{d}\Omega \\ &+\int_\Omega \nabla\times\boldsymbol{A}\cdot\boldsymbol{I}\,\mathrm{d}\Omega,\end{aligned}$$

and

$$\begin{aligned}(12)\quad &F(\boldsymbol{A}) = \frac{1}{2}\int_\Omega \nu\left|\nabla\times\boldsymbol{A}\right|^2 + \nu\left[\nabla\cdot\boldsymbol{A}\right]^2\mathrm{d}\Omega \\ &-\int_\Omega \boldsymbol{A}\cdot\boldsymbol{J}\,\mathrm{d}\Omega + \int_\Omega \nabla\times\boldsymbol{A}\cdot\boldsymbol{I}\,\mathrm{d}\Omega,\end{aligned}$$

when solving the nonlinear equations (8) and (6), respectively.

The value of ν in (2), in case of fixed point method, is selected to be constant [3],

$$(13)\quad \nu = \frac{\nu_{\max}+\nu_{\min}}{2},$$

where $\nu_{\max}$ and $\nu_{\min}$ are the maximum and minimum slope of the characteristics, i.e. the maximum and minimum value of the differential reluctivity $\partial H/\partial B$. The nonlinear residual term $\boldsymbol{I}$ can be arbitrary.

The steps of fixed point iteration are as follows:

1. The solution of (9) or (10) results in the magnetic vector potential $\boldsymbol{A}$. The magnetic flux density is calculated from (3), and the magnetic field intensity is calculated by using the nonlinear model. The nonlinear residual term $\boldsymbol{I}$ updated by using (2) as $\boldsymbol{I} = \boldsymbol{H} - \nu\boldsymbol{B}$.
2. The functional (11) or (12) is calculated.
3. Testing the convergence of the functional. In case of convergence, the iteration is stopped, anyway, it is repeated from step 1 by using the updated residual $\boldsymbol{I}$. Convergence is tested by

$$(14)\quad \frac{F(\boldsymbol{A})-F(\boldsymbol{A}_{last})}{F(\boldsymbol{A}_{last})} \le 10^{-4}.$$

Here $\boldsymbol{A}_{last}$ is the magnetic vector potential in the previous iteration step.

Another scheme can be formulated by using Newton's method on (9) as [2]

$$\begin{aligned}(15)\quad &\int_\Omega \nabla\times\boldsymbol{W}\cdot\left[\nu\,\nabla\times(\boldsymbol{A}+\Delta\boldsymbol{A})\right]\mathrm{d}\Omega = \int_\Omega \nabla\times\boldsymbol{W}\cdot\boldsymbol{T}\,\mathrm{d}\Omega \\ &-\int_\Omega \nabla\times\boldsymbol{W}\cdot\left[\boldsymbol{I}+\left(\frac{\partial H}{\partial B}-\nu\right)\nabla\times\Delta\boldsymbol{A}\right]\mathrm{d}\Omega.\end{aligned}$$

Here $\boldsymbol{A}$, and $\boldsymbol{I}$ are the magnetic vector potential and the residual of the previous iteration step, $\partial H/\partial B$ is the actual slope of the characteristics, and $\Delta\boldsymbol{A}$ is the solution of this equation. The form according to (10) is similar, however the term $\int_\Omega \nabla\cdot\boldsymbol{W}\left[\nu\,\nabla\cdot(\boldsymbol{A}+\Delta\boldsymbol{A})\right]\mathrm{d}\Omega$ has to be appended. The parameter ν is constant, and its value is equal to $\partial H/\partial B$ of the initial step. The first step of iteration is a simple fixed point step ($\nu = \partial H/\partial B$), the others from the second step are:

1. Solving (15) or the equation according to (10), which results in $\Delta\boldsymbol{A}$.
2. Checking the condition $F(\boldsymbol{A}+\Delta\boldsymbol{A}) < F(\boldsymbol{A})$. If it is true, then $\alpha = 1$ is selected. On the contrary, the optimal value of α ($0 < \alpha \le 1$) can be searched by using the golden section search and parabolic interpolation method to find the minimum value of $F(\boldsymbol{A}+\alpha\,\Delta\boldsymbol{A})$.
3. The magnetic vector potential is updated as $\boldsymbol{A} \leftarrow \boldsymbol{A}+\alpha\,\Delta\boldsymbol{A}$, then $\boldsymbol{B}$ is calculated from (3), $\boldsymbol{H}$, and $\partial H/\partial B$ are calculated by using the nonlinear model, then $\boldsymbol{I}$ is updated by (2).
4. The functional (11) or (12) is calculated.
5. Testing the convergence of the functional by (14). The iteration is repeated from step 1, if the iteration step is not convergent.

Simulation of TEAM Problem No. 10

The simulated arrangement can be seen in Fig. 1 [4]. It is a modified version of Problem No. 10 of the TEAM Workshops. The source current flowing in the coil is constant, I= 913.68AT, and I=3000AT.

The nonlinear characteristics of the steel is $\left|\boldsymbol{H}\right| = c\mathrm{e}^{\left|\boldsymbol{B}\right|/\beta-1}$, where $c = 0.0386$, and $\beta = 0.1461$ have been fitted to the measured nonlinear curves in [4].

Three types of mesh have been tried, a coarse, a fine, and a finer mesh containing 2506, 9233, and 16403 finite elements, and the approximation of the magnetic vector potential is second order. Fig. 1 shows the finer mesh of the eighth of the arrangement. It is enough to simulate the eighth of the problem because of symmetry.

The magnetic flux density is driven by the steels, as it can be seen in Fig. 2. Fig. 3 compares the magnetic flux density inside the steel, where the points A, B, C, and D are noted in Fig. 2. It can be seen that the magnetic flux density computed by the formulations are practically identical, however nodal approximation is more sensitive to the density of mesh. It can be concluded that to arrive at accurate flux densities in iron, a fine mesh is necessary in the case of nodal elements. The magnetic flux density has been simulated in the air region along a line close to the horizontal plate, and it can be seen in Fig. 4.

The edge element approximation is much better than the nodal element one. It is noted that only the tangential component of the magnetic vector potential has been set to be continuous in the case of nodal finite element.

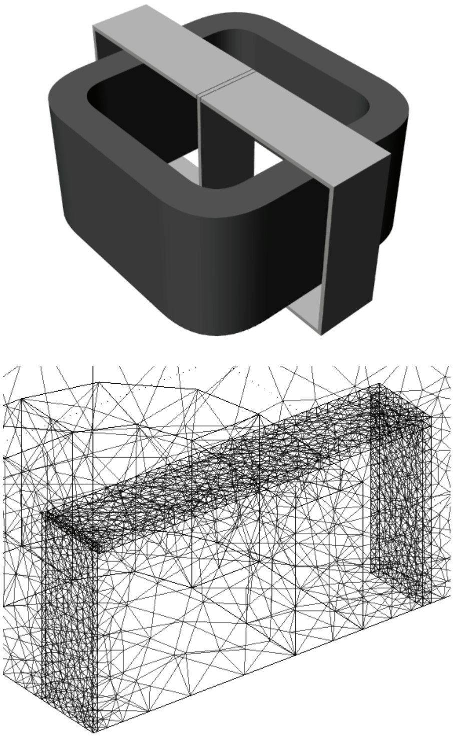

Fig. 1. Steel plates around a coil and its mesh

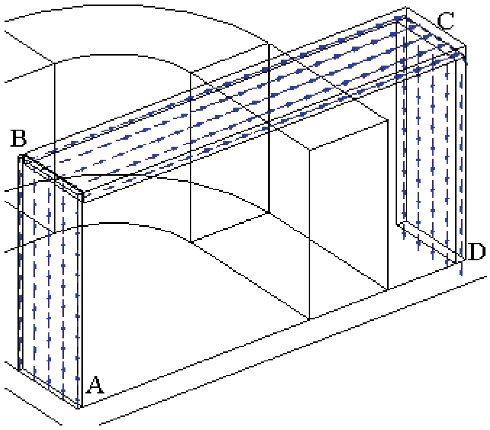

Fig. 2. Magnetic flux is driven by the steels

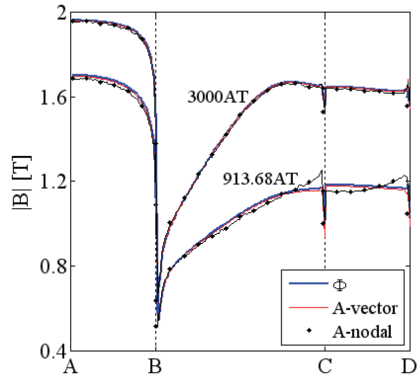

Fig. 3. Comparison of flux in iron

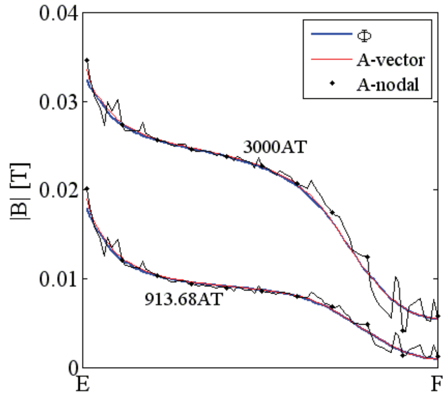

Fig. 4. Comparison of flux in air under the horizontal plate

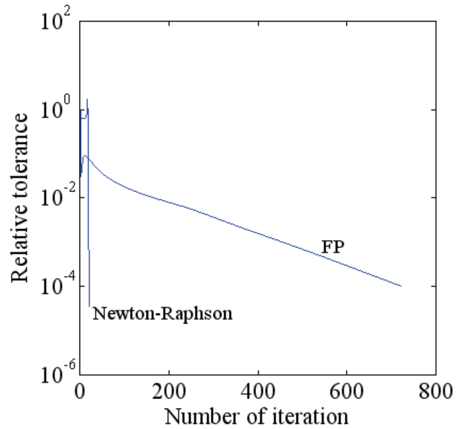

Fig. 5. Comparison of the number of iterations by Newton-Raphson method and the fixed point method

The results have been simulated by using the reduced magnetic scalar potential too, by applying a similar procedure, which can be found in [5].

Simulation of the modified version of TEAM Problem No. 24

This is a modified version of the problemTEAM24, which can be seen in Fig. 6 [6]. The rotor of the arrangement is locked, and the source current of the coils is constant, i.e. a static magnetic field problem has been analyzed.

The nonlinear characteristics of the stator and the rotor is the same as in the last problem.

The number of finite elements is 39060, which results in 55825 and 256530 unknowns for the Φ - formulation (not presented here, refer to [5]) and for the edge element based $\boldsymbol{A}$-formulation, respectively.

The magnetic flux is mainly driven by the stator and the rotor steels as it can be seen in Fig. 7. A comparison between simulated magnetic flux density along a path presented in Fig. 7 is shown in Fig. 8.

Fig. 6. TEAM Problem No. 24

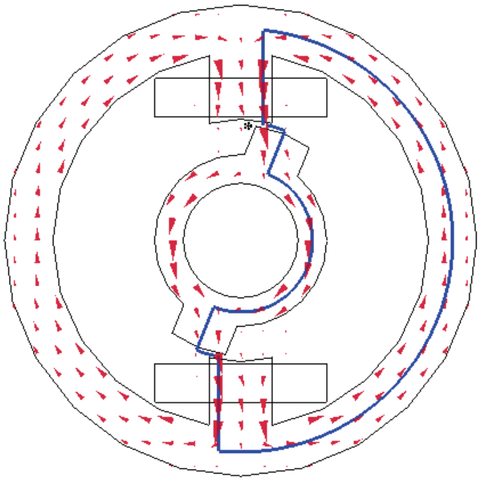

Fig. 7. Magnetic flux is mainly driven by the stator and the rotor

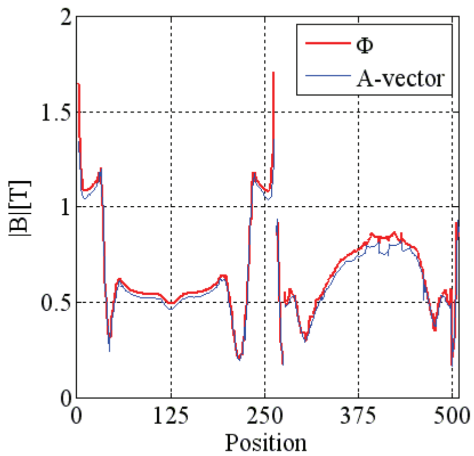

Fig. 8. Magnetic flux density along the path presented in Fig. 7

Conclusion

The proposed combination of the polarization technique and the Newton-Raphson method results in a much faster solver than the fixed point method, especially in the case of vector element representation of $\boldsymbol{A}$. In the case of nodal formulation, under relaxation is almost always necessary, especially when the characteristics is very sharp, and the problem contains singularities.

The aim of further research is to implement the other potential formulations of the static magnetic field problems, and of the eddy current field problems, moreover an applicable hysteresis model based on Preisach's theory. The method must be tested on other problems as well.

Acknowledgments: This paper was supported by the János Bolyai Research Scholarship of the Hungarian Academy of Sciences (BO/00064/06), by Széchenyi István University (15-3201-02), and by the Hungarian Scientific Research Fund (OTKA PD 73242).

REFERENCES

[1] O. Bíró, K. R. Richter, *CAD in Electromagnetism*, in series Advances in Electronics and Electron Physics, Academic Press, New York, 1991.

[2] J. Saitz, Newton-Raphson Method and Fixed-Point Technique in Finite Element Computation of Magnetic Field Problems in Media with Hysteresis, *IEEE Trans. on Magn.*, vol. 35, 1999, pp. 1398-1401.

[3] I. F. Hantila, Mathematical model of the relation between *B* and *H* for nonlinear media, *Revue Roumaine Des Sciences Techniques, Electrotechnique et Energetique*, Bucarest, 1974, pp. 429-448.

[4] T. Nakata and K. Fujiwara. Summary of results for benchmark problem 10 (steel plates around a coil), *European TEAM Workshop and International Seminar on Electromagnetic Analysis*, Oxford, 1990.

[5] M. Kuczmann, Handling Nonlinearity by the Polarization Method and the Newton-Raphson Technique, submitted to the 13th IGTE Symposium, Graz, Austria, 2008.

[6] N. Allen, and D. Rodger, "Description of TEAM Workshop Problem 24: Nonlinear time-transient rotational test rig," 1996.

***Authors**: Dr. Miklós Kuczmann, PhD, Associate Professor, Széchenyi István University, Department of Telecommunications, Laboratory of Electromagnetic Fields, Egyetem tér 1, H-9026 Győr, Hungary, E-mail: kuczmann@sze.hu.*